
Abstract

Printing technology has been extensively investigated, with the majority of that investigation historically based upon applications to the two-dimensional printing industry. Recently, however, it has spread to numerous new application areas, including electronics packaging, optics, and additive manufacturing. Some of these applications, in fact, have literally taken the technology into a new dimension. The employment of printing technologies in the creation of three-dimensional products has quickly become an extremely promising manufacturing practice, both widely studied and increasingly widely used.

This chapter will summarize the printing achievements made in the additive manufacturing industry and in academia. The development of printing as a process to fabricate 3D parts is summarized, followed by a survey of commercial polymer printing machines. The focus of this chapter is on material jetting (MJ) in which all of the part material is dispensed from a print head. This is in contrast to binder jetting, where binder or other additive is printed onto a powder bed which forms the bulk of the part. Binder jetting is the subject of Chap. 8. Some of the technical challenges of printing are introduced; material development for printing polymers, metals, and ceramics is investigated in some detail. Models of the material jetting process are introduced that relate pressure required to fluid properties. Additionally, a printing indicator expression is derived and used to analyze printing conditions.

7.1 Evolution of Printing as an Additive Manufacturing Process

Two-dimensional inkjet printing has been in existence since the 1960s, used for decades as a method of printing documents and images from computers and other digital devices. Inkjet printing is now widely used in the desktop printing industry,

commercialized by companies such as HP and Canon. Le [1] provides a thorough review of the historical development of the inkjet printing industry.

Printing as a three-dimensional building method was first demonstrated in the 1980s with patents related to the development of Ballistic Particle Manufacturing, which involved simple deposition of “particles” of material onto an article [2]. The first commercially successful technology was the ModelMaker from Sanders Prototype (now Solidscape), introduced in 1994, which printed a basic wax material that was heated to liquid state [3]. In 1996, 3D Systems joined the competition with the introduction of the Actua 2100, another wax-based printing machine. The Actua was revised in 1999 and marketed as the ThermoJet [3]. In 2001, Sanders Design International briefly entered the market with its Rapid ToolMaker, but was quickly restrained due to intellectual property conflicts with Solidscape [3]. It is notable that all of these members of the first generation of RP printing machines relied on heated waxy thermoplastics as their build material; they are therefore most appropriate for concept modeling and investment casting patterns.

More recently, the focus of development has been on the deposition of acrylate photopolymer, wherein droplets of liquid monomer are formed and then exposed to ultraviolet light to promote polymerization. The reliance upon photopolymerization is similar to that in stereolithography, but other process challenges are significantly different. The leading edge of this second wave of machines arrived on the market with the Quadra from Objet Geometries of Israel in 2000, followed quickly by the revised QuadraTempo in 2001. Both machines jetted a photopolymer using print heads with over 1,500 nozzles [3]. In 2003, 3D Systems launched a competing technology with its InVision 3D printer. Multi-Jet Modeling, the printing system used in this machine, was actually an extension of the technology developed with the ThermoJet line [3], despite the change in material solidification strategy. The companies continue to innovate, as will be discussed in the next sections.

7.2 Materials for Material Jetting

While industry players have so far introduced printing machines that use waxy polymers and acrylic photopolymers exclusively, research groups around the world have experimented with the potential for printing machines that could build in those and other materials. Among those materials most studied and most promising for future applications are polymers, ceramics, and metals. In addition to the commercially available materials, this section highlights achievements in related research areas.

For common droplet formation methods, the maximum printable viscosity threshold is generally considered to be in the range of 20–40 centipoise (cP) at the printing temperature [4–6]. An equivalent unit of measure is the milli-Pascal-second, denoted mPa s if SI units are preferred. To facilitate jetting, materials that are solid at room temperature must be heated so that they liquefy. For high viscosity fluids, the viscosity of the fluid must be lowered to enable jetting. The most common practices are to use heat or solvents or other low viscosity components

in the fluid. In addition to these methods, it is also possible that in some polymer deposition cases shear thinning might occur, dependent upon the material or solution in use; drop-on-demand (DOD) printers are expected to produce strain rates of 10^3 – 10^4 , which should be high enough to produce shear-thinning effects [4, 7]. While other factors such as liquid density or surface tension and print head or nozzle design may affect the results, the limitation on viscosity quickly becomes the most problematic aspect for droplet formation in material jetting.

7.2.1 Polymers

Polymers consist of an enormous class of materials, representing a wide range of mechanical properties and applications. And although polymers are the only material currently used in commercial AM machines, there seems to be relatively little discussion on polymer inkjet production of macro three-dimensional structures in the published scientific literature.

Gao and Sonin [8] present the first notable academic study of the deposition and solidification of groups of molten polymer microdrops. They discuss findings related to three modes of deposition: columnar, sweep (linear), and repeated sweep (vertical walls). The two materials used in their investigations were a candelilla wax and a microcrystalline petroleum wax, deposited in droplets 50 μm in diameter from a print head 3–5 mm from a cooled substrate. The authors first consider the effects of droplet deposition frequency and cooling on columnar formation. As would be expected, if the drops are deposited rapidly (≥ 50 Hz in this case), the substrate on which they impinge is still at an elevated temperature, reducing the solidification contact angle and resulting in ball-like depositions instead of columns (Fig. 7.1a). Numerical analyses of the relevant characteristic times of cooling are included. Gao and Sonin also consider horizontal deposition of droplets and the subsequent formation of lines. They propose that smooth solid lines will be formed only in a small range of droplet frequencies, dependent upon the sweep speed, droplet size, and solidification contact angle (Fig. 7.1b). Finally, they propose that wall-like deposition will involve a combination of the relevant aspects from each of the above situations.

Reis et al. [9] also provide some discussion on the linear deposition of droplets. They deposited molten Mobilwax paraffin wax with a heated print head from SolidScape. They varied both the print head horizontal speed and the velocity of droplet flight from the nozzle. For low droplet speeds, low sweep speeds created discontinuous deposition and high sweep speeds created continuous lines (Fig. 7.2a–c). High droplet impact speed led to splashing at high sweep speeds and line gulges at low sweep speeds (Fig. 7.2d–f).

From these studies, it is clear that process variables such as print head speed, droplet velocity, and droplet frequency affect the quality of the deposit. These process variables vary depending upon the characteristics of the fluid being printed, so some process development, or fine-tuning, is generally required when trying to print a new material or develop a new printing technology.

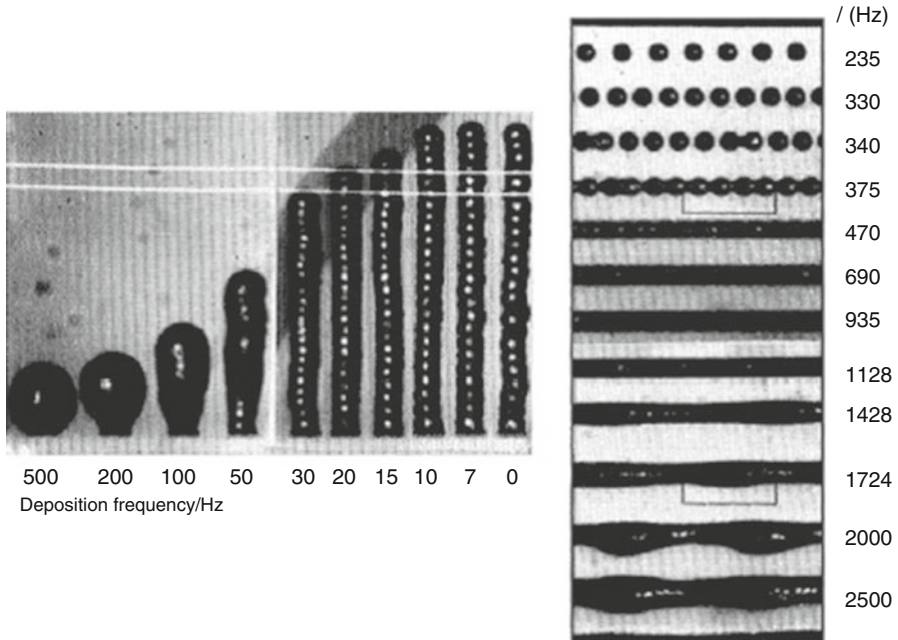


Fig. 7.1 (a) Columnar formation and (b) line formation as functions of droplet impingement frequency [8]

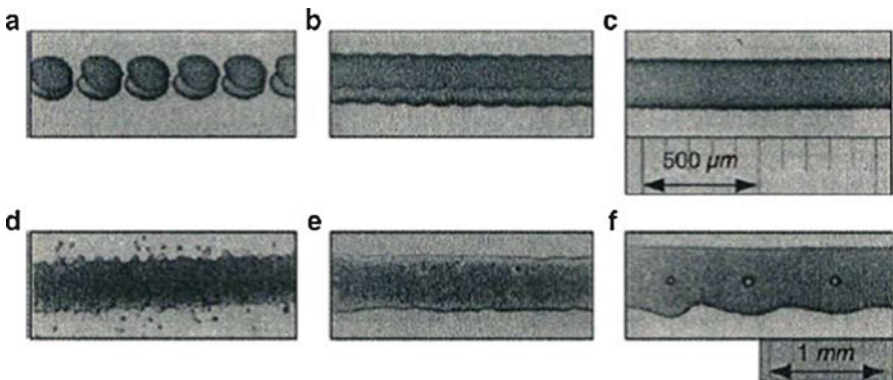
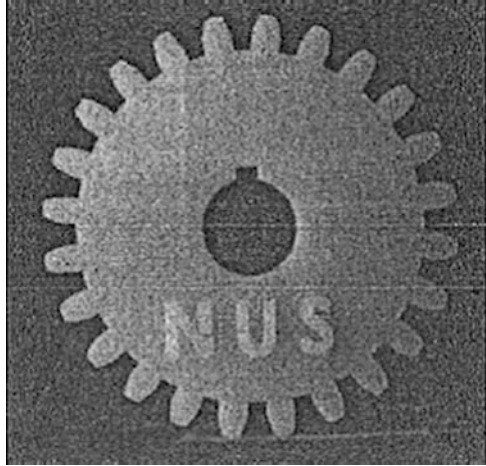


Fig. 7.2 Results of varying sweep and impact speeds [9]

Feng et al. [10] finally present a full system, based on a print head from MicroFab Technologies Inc. that functions similarly to the commercially available machines. It prints a wax material which is heated to 80 °C, more than 10° past its melting point, and deposits it in layers 13–60 μm thick. The deposition pattern is controlled by varying the droplet size and velocity, as well as the pitch and hatch

Fig. 7.3 Wax gear [10]

spacing of the lines produced. An example of the result, a 2.5-dimensional gear, is presented in Fig. 7.3.

The earliest and most often used solution to the problem of high viscosity is to heat the material until its viscosity drops to an acceptable point. As discussed in Sect. 7.5, for example, commercial machines such as 3D Systems' ThermoJet and Solidscape's T66 all print proprietary thermoplastics, which contain mixtures of various waxes and polymers that are solid at ambient temperatures but convert to a liquid phase at elevated printing temperatures [11]. In developing their hot melt materials, for example, 3D Systems investigated various mixtures consisting of a low shrinkage polymer resin, a low viscosity material such as paraffin wax, a microcrystalline wax, a toughening polymer, and a small amount of plasticizer, with the possible additions of antioxidants, coloring agents, or heat dissipating filler [12]. These materials were formulated to have a viscosity of 18–25 cP and a surface tension of 24–29 dyn/cm at the printing temperature of 130 °C. De Gans et al. [13] contend that they have used a micropipette optimized for polymer printing applications that was able to print Newtonian fluids with viscosities up to 160 cP.

The most recent development in addressing the issues of viscosity is the use of prepolymers in the fabrication of polymer parts. This is the method currently employed by the two newest commercially available machine lines, as discussed in Sect. 7.5. For example, 3D Systems investigated a series of UV-curable printing materials, consisting of mixtures of high-molecular weight monomers and oligomers such as urethane acrylate or methacrylate resins, urethane waxes, low molecular weight monomers and oligomers such as acrylates or methacrylates that function as diluents, a small amount of photoinitiators, and other additives such as stabilizers, surfactants, pigments, or fillers [14, 15]. These materials also benefited from the effects of hot melt deposition, as they were printed at a temperature of 70–95 °C, with melting points between 45 and 65 °C. At the printing temperatures, these materials had a viscosity of about 10–16 cP.

One problem encountered, and the reason that the printing temperatures cannot be as high as those used in hot melt deposition, is that when kept in the heated state for extended periods of time, the prepolymers begin to polymerize, raising the viscosity and possibly clogging the nozzles when they are finally printed [15]. Another complication is that the polymerization reaction, which occurs after printing, must be carefully controlled to assure dimensional accuracy.

7.2.2 Ceramics

One significant advance in terms of direct printing for three-dimensional structures has been achieved in the area of ceramic suspensions. As in the case of polymers, studies have been conducted that investigate the basic effects of modifying sweep speed, drop-to-drop spacing, substrate material, line spacing, and simple multilayer forms in the deposition of ceramics [16]. These experiments were conducted with a mixture of zirconia powder, solvent, and other additives, which was printed from a 62 μm nozzle onto substrates 6.5 mm away. The authors found that on substrates that permitted substantial spreading of the deposited materials, neighboring drops would merge to form single, larger shapes, whereas on other substrates the individual dots would remain independent (see Fig. 7.4). In examples where multiple layers were printed, the resulting deposition was uneven, with ridges and valleys throughout.

A sizable body of work has been amassed in which suspensions of alumina particles are printed via a wax carrier [4] which is melted by the print head. Suspensions of up to 40 % solids loading have been successfully deposited at viscosities of 2.9–38.0 cP at a measurement temperature of 100 °C; higher concentrations of the suspended powder have resulted in prohibitively high viscosities. Because this deposition method results in a part with only partial ceramic density, the green part must be burnt out and sintered, resulting in a final product which is 80 % dense but whose dimensions are subject to dramatic shrinkage [17]. A part created in this manner is shown in Fig. 7.5.

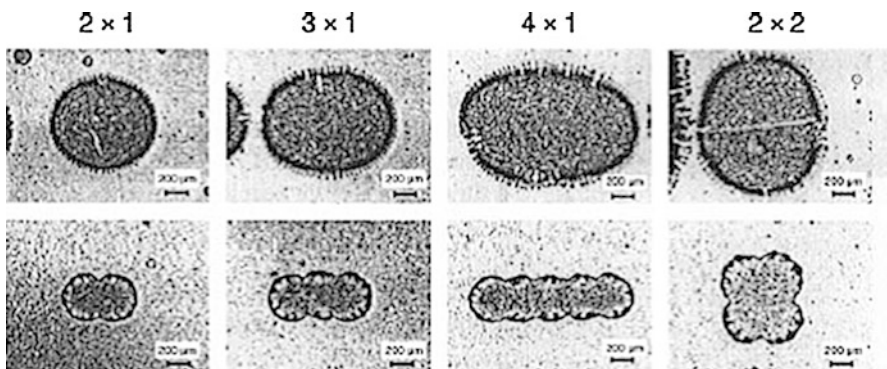


Fig. 7.4 Droplets on two different substrates [16]

Fig. 7.5 Sintered alumina impeller [17]

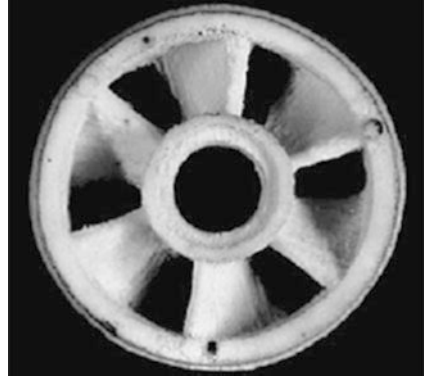
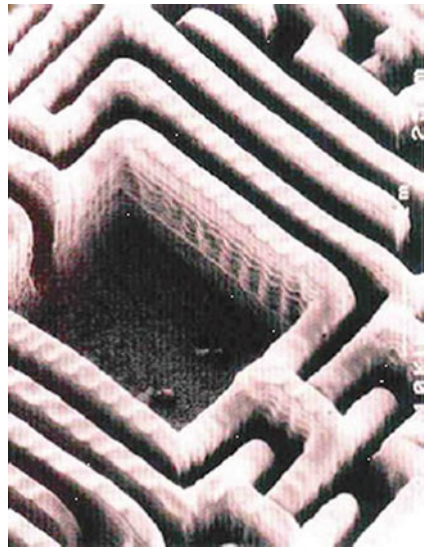


Fig. 7.6 Sintered zirconia vertical walls [18]



Similar attempts have been made with zirconia powder, using material with 14 % ceramic content by volume [18], with an example shown in Fig. 7.6, as well as with PZT, up to 40 % ceramic particles by volume [19].

7.2.3 Metals

Much of the printing work related to metals has focused upon the use of printing for electronics applications—formation of traces, connections, and soldering. Liu and Orme [20] present an overview of the progress made in solder droplet deposition for the electronics industry. Because solder has a low melting point, it is an obvious choice as a material for printing. They reported use of droplets of 25–500 μm , with

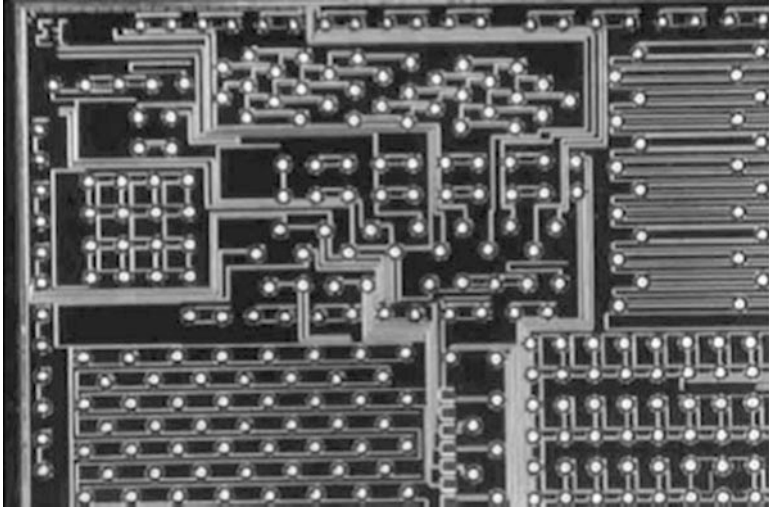


Fig. 7.7 IC test board with solder droplets [20]

results such as the IC test board in Fig. 7.7, which has 70 μm droplets of Sn63/Pb37. In related work, a solder was jetted whose viscosity was approximately 1.3 cP, continuously jetted under a pressure of 138 kPa. Many of the results to which they refer are those of researchers at MicroFab Technologies, who have also produced solder forms such as 25 μm diameter columns.

There is, however, some work in true three-dimensional fabrication with metals. Priest et al. [21] provide a survey of liquid metal printing technologies and history, including alternative technologies employed and ongoing research initiatives. Metals that had been printed included copper, aluminum, tin, various solders, and mercury. One major challenge identified for depositing metals is that the melting point of the material is often high enough to significantly damage components of the printing system.

Orme et al. [22, 23] report on a process that uses droplets of Rose's metal (an alloy of bismuth, lead, and tin). They employ nozzles of diameter 25–150 μm with resulting droplets of 47–283 μm . In specific cases, parts with porosity as low as 0.03 % were formed without post-processing, and the microstructure formed is more uniform than that of standard casting. In discussion of this technology, considerations of jet disturbance, aerodynamic travel, and thermal effects are all presented.

Yamaguchi et al. [24, 25] used a piezoelectrically driven actuator to deposit droplets of an alloy (Bi–Pb–Sn–Cd–In), whose melting point was 47 $^{\circ}\text{C}$. They heated the material to 55 $^{\circ}\text{C}$ and ejected it from nozzles 200 μm , 50 μm , and less than 8 μm in diameter. As expected, the finer droplets created parts with better resolution. The density, or “packing rate,” of some parts reached 98 %. Other examples of fabricated parts are shown in Fig. 7.8.

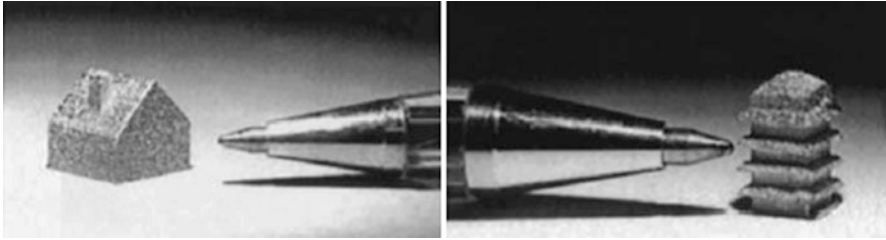


Fig. 7.8 Examples of parts fabricated with metal printing [25]

More recently, several research groups have demonstrated aluminum deposition [26, 27]. In one example, near-net shape components, with fairly simple shapes, have been formed from Al2024 alloy printed from a 100 μm orifice. In another example, pressure pulses of argon gas in the range of 20–100 kPa were used to eject droplets of molten aluminum at the rate of 1–5 drops per second. To achieve this, the aluminum was melted at 750 $^{\circ}\text{C}$ and the substrate to 300 $^{\circ}\text{C}$. The nozzle orifice used was 0.3 mm in diameter, with a resulting droplet size of 200–500 μm and a deposited line of width 1.00 mm and thickness 0.17 mm. The final product was a near-net shape part of density up to 92 %.

As these examples have shown, printing is well on its way to becoming a viable process for three-dimensional prototyping and manufacturing. While industry has only barely begun to use printing in this arena, the economic and efficiency advantages that printing provide ensure that it will be pursued extensively in the future. Researchers in academia have expanded the use of printing to materials such as ceramics and metals, thus providing additional prospective applications for the technology. Despite its great potential, however, the growth of printing has been hampered significantly by technical challenges inherent to the printing process. These challenges and possible solutions are investigated in subsequent sections.

7.2.4 Solution- and Dispersion-Based Deposition

As hot melt deposition has very specific requirements for the material properties of what is printed, many current applications have turned to solution- or dispersion-based deposition. This allows the delivery of solids or high-molecular weight polymers in a carrier liquid of viscosity low enough to be successfully printed. De Gans et al. [5] provided a review of a number of polymeric applications in which this strategy is employed.

A number of investigators have used solution and dispersion techniques in accurate deposition of very small amounts of polymer in thin layers for mesoscale applications, such as polymer light-emitting displays, electronic components, and surface coatings and masks. For example, Shimoda et al. [28] present a technique to develop light-emitting polymer diode displays using inkjet deposition of conductive polymers. Three different electroluminescent polymers (polyfluorine and two

derivatives) were printed in organic solvents at 1–2 wt%. As another example, De Gans et al. [5] report a number of other results related to the creation of polymer light-emitting displays: a precursor of poly(*p*-phenylene vinylene) (PPV) was printed as a 0.3 wt% solution; and PPV derivatives were printed in 0.5–2.0 wt% solutions in solvents such as tetraline, anisole, and *o*-xylene. Such low weight percentages are typical.

In deposition of ceramics, the use of a low viscosity carrier is also a popular approach. Tay and Edirisinghe [16], for example, used ceramic powder dispersed in industrial methylated spirit with dispersant, binder, and plasticizer additives resulting in a material that was 4.5 % zirconia by volume. The resulting material had a viscosity of 3.0 cP at 20 °C and a shear rate of 1,000 s⁻¹. Zhao et al. [29] tested various combinations of zirconia and wax carried in octane and isopropyl alcohol, with a dispersant added to reduce sedimentation. The viscosities of these materials were 0.6–2.9 cP at 25 °C; the one finally selected was 14.2 % zirconia by volume.

Despite the success of solution and dispersion deposition for these specific applications, however, there are some serious drawbacks, especially in considering the potential for building complex, large, 3D components. The low concentrations of polymer and solid used in the solutions and dispersions will restrict the total amount of material that can be deposited. Additionally, it can be difficult to control the deposition pattern of this material within the area of the droplet's impact. Shimoda et al. [28], among others, report the formation of rings of deposited material around the edge of the droplet. They attribute this to the fact that the contact line of the drying drop is pinned on the substrate. As the liquid evaporates from the edges, it is replenished from the interior, carrying the solutes to the edge. They contend that this effect can be mitigated by control of the droplet drying conditions.

Another difficulty with solutions or dispersions, especially those based on volatile solvents, is that use of these materials can result in precipitations forming in the nozzle after a very short period of time [13], which can clog the nozzle, making deposition unreliable or impossible.

7.3 Material Processing Fundamentals

7.3.1 Technical Challenges of MJ

As evidenced by the industry and research applications discussed in the previous section, material jetting already has a strong foothold in terms of becoming a successful AM technology. There are, however, some serious technical shortcomings that have prevented its development from further growth. To identify and address those problems, the relevant phenomena and strategic approaches taken by its developers must be understood. In the next two sections, the technical challenges of the printing process are outlined, the most important of its limitations

relevant to the deposition of functional polymers are identified, and how those limitations are currently addressed is summarized.

Jetting for three-dimensional fabrication is an extremely complex process, with challenging technical issues throughout. The first of these challenges is formulation of the liquid material. If the material is not in liquid form to begin with, this may mean suspending particles in a carrier liquid, dissolving materials in a solvent, melting a solid polymer, or mixing a formulation of monomer or prepolymer with a polymerization initiator. In many cases, other substances such as surfactants are added to the liquid to attain acceptable characteristics. Entire industries are devoted to the mixture of inks for two-dimensional printing, and it is reasonable to assume that in the future this will also be the case for three-dimensional fabrication.

The second hurdle to overcome is droplet formation. To use inkjet deposition methods, the material must be converted from a continuous volume of liquid into a number of small discrete droplets. This function is often dependent upon a finely tuned relationship between the material being printed, the hardware involved, and the process parameters; a number of methods of achieving droplet formation are discussed in this section. Small changes to the material, such as the addition of tiny particles [30], can dramatically change its droplet forming behavior as well, as can changes to the physical setup.

A third challenge is control of the deposition of these droplets; this involves issues of droplet flight path, impact, and substrate wetting or interaction [31–35]. In printing processes, either the print head or the substrate is usually moving, so the calculation of the trajectory of the droplets must take this issue into account. In addition to the location of the droplets' arrival, droplet velocity and size will also affect the deposition characteristics and must be measured and controlled via nozzle design and operation [36]. The quality of the impacted droplet must also be controlled: if smaller droplets, called satellites, break off from the main droplet during flight, then the deposited material will be spread over a larger area than intended and the deposition will not have well-defined boundaries. In the same way, if the droplet splashes on impact, forming what is called a "crown," similar results will occur [37]. All of the effects will negatively impact the print quality of the printed material.

Concurrently, the conversion of the liquid material droplets to solid geometry must be carefully controlled; as discussed in Sect. 7.2, material jetting relies on a phase change of the printed material. Examples of phase change modes employed in existing printing technologies are: solidification of a melted material (e.g., wax, solder), evaporation of the liquid portion of a solution (e.g., some ceramic approaches), and curing of a photopolymer (e.g., Objet, ProJet machines) or other chemical reactions. The phase change must occur either during droplet flight or soon after impact; the time and place of this conversion will also affect the droplet's interaction with the substrate [38, 39] and the final deposition created. To further complicate the matter, drops may solidify nonuniformly, creating warpage and other undesirable results [40].

An additional challenge is to control the deposition of droplets on top of previously deposited layers, rather than only upon the initial substrate

[8, 16]. The droplets will interact differently, for example, with a metal plate substrate than with a surface of previously printed wax droplets. To create substantive three-dimensional parts, each layer deposited must be fully bound to the previous layer to prevent delamination, but must not damage that layer while being created. Commercially available machines tend to approach this problem by employing devices that plane or otherwise smooth the surface periodically [40–42].

Operational considerations also pose a challenge in process planning for MJ. For example, because nozzles are so small, they often clog, preventing droplets from exiting. Much attention has been given to monitoring and maintaining nozzle performance during operation [40]. Most machines currently in use go through purge and cleaning cycles during their builds to keep as many nozzles open as possible; they may also wipe the nozzles periodically [41]. Some machines may also employ complex sensing systems to identify and compensate for malfunctioning or inconsistent nozzles [43, 44]. In addition, many machines, including all commercial AM machines, have replaceable nozzles in case of permanent blockage.

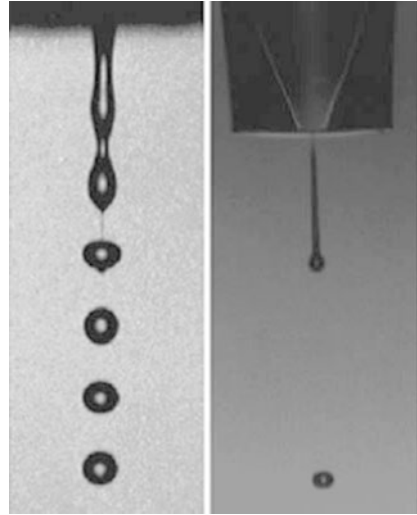
Finally, to achieve the best print resolution, it is advantageous to produce many small droplets very close together. However, this requires high nozzle density in the print head, which is unattainable for many nozzle manufacturing processes. An alternative to nozzle density is to make multiple passes over the same area, effectively using process planning instead of hardware to create the desired effect [41]. Even in cases where high nozzle density is possible, however, problems arise due to crosstalk—basically an “overlapping” of the thermal or pressure differentials used to drive adjacent nozzles.

In approaching a printing process, these numerous challenges must in some sense be addressed sequentially: flight pattern cannot be studied until droplets are formed and layering cannot be investigated until deposition of single droplets is controlled. In terms of functional polymer deposition, the challenge of material preparation has effectively been addressed; numerous polymer resins and mixtures already exist. It is the second challenge—droplet formation—that is therefore the current limiting factor in deposition of these materials. To understand these limitations, Sect. 7.3.2 reviews the dynamic processes that are currently used to form droplets and Sect. 7.2 considered necessary methods of modifying the jetting material for use with those processes.

7.3.2 Droplet Formation Technologies

Over the time that two-dimensional inkjet printing has evolved, a number of methods for creating and expelling droplets have been developed. The main distinction in categorizing the most common of technologies refers to the possible modes of expulsion: continuous stream (CS) and DOD. This distinction refers to the form in which the liquid exits the nozzle—as either a continuous column of liquid or as discrete droplets. Figure 7.9 shows the distinction between continuous (left) and DOD (right) formations.

Fig. 7.9 Continuous (*left*) and drop-on-demand (*right*) deposition [46]



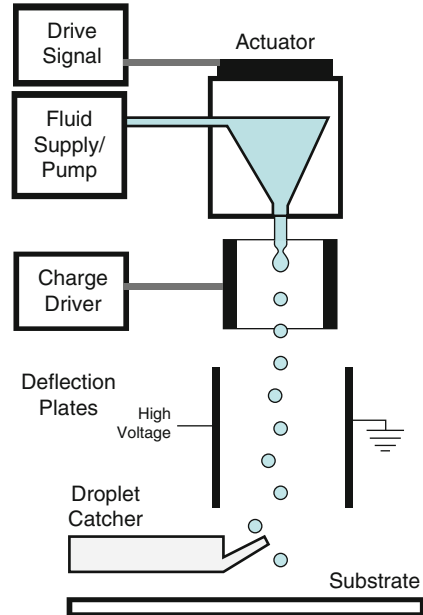
7.3.3 Continuous Mode

In CS mode, a steady pressure is applied to the fluid reservoir, causing a pressurized column of fluid to be ejected from the nozzle. After departing the nozzle, this stream breaks into droplets due to Rayleigh instability. The breakup can be made more consistent by vibrating, perturbing, or modulating the jet at a fixed frequency close to the spontaneous droplet formation rate, in which case the droplet formation process is synchronized with the forced vibration, and ink droplets of uniform mass are ejected [45]. Because droplets are produced at constant intervals, their deposition must be controlled after they separate from the jet. To achieve this, they are introduced to a charging field and thus attain an electrostatic charge. These charged particles then pass through a deflection field, which directs the particles to their desired destinations—either a location on the substrate or a container of material to be recycled or disposed. Figure 7.10 shows a schematic of the function of this type of binary deflection continuous system.

An advantage of CS deposition is the high throughput rate; it has therefore seen widespread use in applications such as food and pharmaceutical labeling [5]. Two major constraints related to this method of droplet formation are, however, that the materials must be able to carry a charge and that the fluid deflected into the catcher must be either disposed of or reprocessed, causing problems in cases where the fluid is costly or where waste management is an issue.

In terms of droplets formed, commercially available systems typically generate droplets that are about 150 μm in diameter at a rate of 80–100 kHz, but frequencies of up to 1 MHz and droplet sizes ranging from 6 μm (10 fL) to 1 mm (0.5 μL) have been reported [46]. It has also been shown that, in general, droplets formed from continuous jets are almost twice the diameter of the undisturbed jet [47].

Fig. 7.10 Binary deflection continuous printing [46]



A few investigators of three-dimensional deposition have opted to use continuous printing methods. Blazdell et al. [48] used a continuous printer from Biodot, which was modulated at 66 kHz while ejecting ceramic ink from 50 and 75 μm nozzles. They used 280 kPa of air pressure. Blazdell [49] reports later results in which this Biodot system was modulated at 64 kHz, using a 60 μm nozzle that was also 60 μm in length. For much of the development of the 3D Printing binder jetting process, CS deposition was used. At present, the commercial machines based on 3DP (from 3D Systems and Ex One) use standard DOD print heads. In metal fabrication, Tseng et al. [50] used a continuous jet in depositing their solder alloy, which had a viscosity of about 2 cP at the printing temperature. Orme et al. [22, 23] also report the use of an unspecified continuous system in deposition of solders and metals.

7.3.4 DOD Mode

In DOD mode, in contrast, individual droplets are produced directly from the nozzle. Droplets are formed only when individual pressure pulses in the nozzle cause the fluid to be expelled; these pressure pulses are created at specific times by thermal, electrostatic, piezoelectric, acoustic, or other actuators [1]. Figure 7.11 shows the basic functions of a DOD setup. Liu and Orme [20] assert that DOD methods can deposit droplets of 25–120 μm at a rate of 0–2,000 drops per second.

In the current DOD printing industry, thermal (bubble-jet) and piezoelectric actuator technologies dominate; these are shown in Fig. 7.12. Thermal actuators

Fig. 7.11 Schematic of drop-on-demand printing system [46]

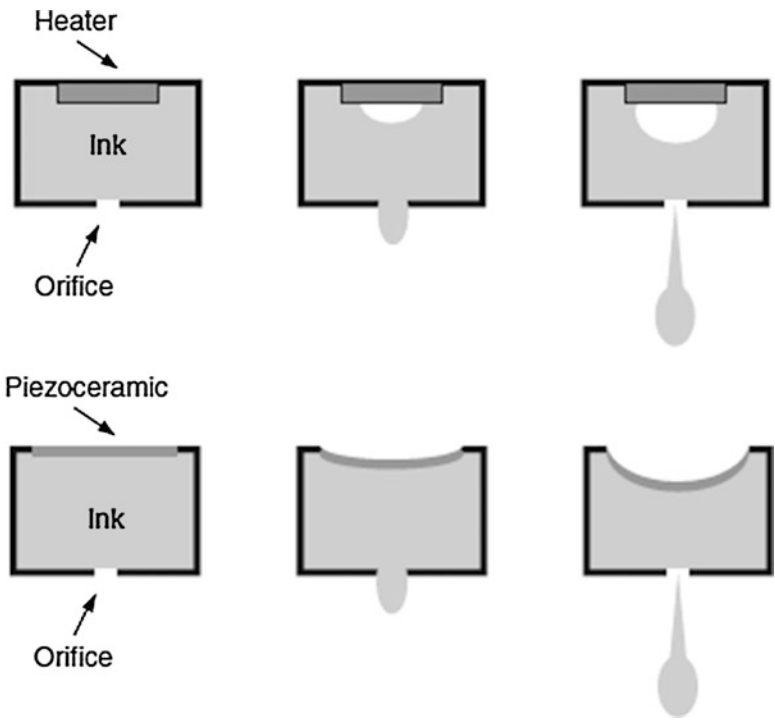
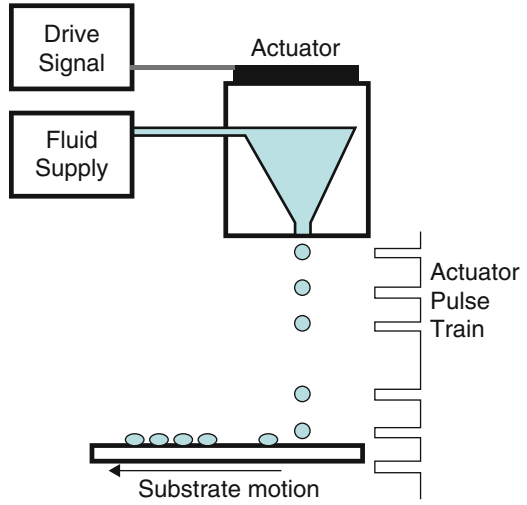


Fig. 7.12 Thermal (*top*) and piezoelectric (*bottom*) DOD ejection

rely on a resistor to heat the liquid within a reservoir until a bubble expands in it, forcing a droplet out of the nozzle. Piezoelectric actuators rely upon the deformation of a piezoelectric element to reduce the volume of the liquid reservoir, which causes a droplet to be ejected. As noted by Basaran [51], the waveforms employed in piezoelectrically driven DOD systems can vary from simple positive square waves to complex negative–positive–negative waves in which the amplitude, duration, and other parameters are carefully modulated to create the droplets as desired.

In their review of polymer deposition, De Gans et al. [5] assert that DOD is the preferable method for all applications that they discuss due to its smaller drop size (often of diameter similar to the orifice) and higher placement accuracy in comparison to CS methods. They further argue that piezoelectric DOD is more widely applicable than thermal because it does not rely on the formation of a vapor bubble or on heating that can damage sensitive materials.

The preference for piezoelectrically driven DOD printing is reflected in the number of investigators who use and study such setups. For example, Gao and Sonin [8] use this technology to deposit 50 μm droplets of two waxes, whose viscosity at 100 $^{\circ}\text{C}$ is about 16 cP. Siringhaus et al. [52] and Shimoda et al. [28] both use piezoelectric DOD deposition for polymer solutions, as discussed in Sect. 7.2.1. In ceramic deposition, Reis et al. [9] print mixtures with viscosities 6.5 and 14.5 cP at 100 $^{\circ}\text{C}$ and frequencies of 6–20 kHz. Yamaguchi et al. [24, 25] also used a piezoelectrically driven DOD device at frequencies up to 20 Hz in the deposition of metal droplets. Similarly, the solder droplets on the circuit board in Fig. 7.7 were also deposited with a DOD system.

At present, all commercial AM printing machines use DOD print heads, generally from a major manufacturer of printers or printing technologies. Such companies include Hewlett-Packard, Canon, Dimatix, Konica-Minolta, and Xaar.

7.3.5 Other Droplet Formation Methods

Aside from the standard CS and DOD methods, other technologies have been experimentally investigated but have not enjoyed widespread use in industry applications. Liquid spark jetting, a relative of thermal printing, relies on an electrical spark discharge instead of a resistor to form a gas bubble in the reservoir [45, 52]. The electrohydrodynamic inkjet employs an extremely powerful electric field to pull a meniscus and, under very specific conditions, droplets from a pressure-controlled capillary tube; these droplets are significantly smaller than the tube from which they emanate. Electro-rheological fluid jetting uses an ink whose properties change under high electric fields; the fluid flows only when the electric field is turned off [53]. In their flextensional ultrasound droplet ejectors, Percin and Khuri-Yakub [54] demonstrate both DOD and continuous droplet formation with a system in which a plate containing the nozzle orifice acts as the actuator, vibrating at resonant frequencies and forming droplets by creating capillary waves on the liquid surface as well as an increased pressure in the liquid. Focused acoustic beam

ejection uses a lens to focus an ultrasound beam onto the free surface of a fluid, using the acoustic pressure transient generated by the focused tone burst to eject a fluid droplet [55]. Meacham et al. extended this work [56] to develop an inexpensive ultrasonic droplet generator and developed a fundamental understanding of its droplet formation mechanisms [57]. These ultrasonic droplet generators show promise in ejecting viscous polymers [58]. Fukumoto et al. [59] present a variant technology in which ultrasonic waves are focused onto the surface of the liquid, forming surface waves that eventually break off into a mist of small droplets. Overviews of these various droplet formation methods are given by Lee [53] and Basaran [51].

Summary: While the general challenges of material jetting for three-dimensional fabrication are identified, there are many aspects that are not well or fully understood. Open research questions abound in almost all stages of the printing process—droplet formation, deposition control, and multilayer accumulation. For the case of polymer jetting, the most appropriate limitation to address is that of droplet formation. Because systems developed for inviscid materials are being used for these applications, numerous accommodations and limitations currently exist; users commonly handle this by modifying the materials to fit the requirements of the existing hardware. However, if the method of droplet formulation could be modified instead, this might allow the deposition of a wider range of materials. A recently developed acoustic focusing ultrasonic droplet generator, under investigation at Georgia Institute of Technology, employs a strategy different from those of existing technologies, which may provide the capabilities to fulfill this need [60].

7.4 MJ Process Modeling

Conservation of energy concepts provides an appropriate context for investigating droplet generation mechanisms for printing. Essentially, the energy imparted by the actuation method to the liquid must be sufficient to balance three requirements: fluid flow losses, surface energy, and kinetic energy. The losses originate from a conversion of kinetic energy to thermal energy due to the viscosity of the fluid within the nozzle; this conversion can be thought of as a result of internal friction of the liquid. The surface energy requirement is the additional energy needed to form the free surface of the droplet or jet. Finally, the resulting droplet or jet must still retain enough kinetic energy to propel the liquid from the nozzle towards the substrate. This energy conservation can be summarized as

$$E_{\text{imparted}} = E_{\text{loss}} + E_{\text{surface}} + E_{\text{kinetic}} \quad (7.1)$$

The conservation law can be considered in the form of actual energy calculations or in the form of pressure, or energy per unit volume, calculations. For example, Sweet used the following approximation for the gauge pressure required in the reservoir of a continuous jetting system [61]:

$$\Delta p = 32\mu d_j^2 v_j \int_{l_1}^{l_2} \frac{dl}{d_n^4} + \frac{2\sigma}{d_j} + \frac{\rho v_j^2}{2} \quad (7.2)$$

where, Δp is the total gauge pressure required, μ is the dynamic viscosity of the liquid, ρ is the liquid's density, σ is the liquid's surface tension, d_j is the diameter of the resultant jet, d_n is the inner diameter of the nozzle or supply tubing, v_j is the velocity of the resultant jet, and l is the length of the nozzle or supply tubing. The first term on the right of (7.2) is an approximation of the pressure loss due to viscous friction within the nozzle and supply tubing. The second term is the internal pressure of the jet due to surface tension and the third term is the pressure required to provide the kinetic energy of the droplet or jet.

Energy conservation can also be thought of as a balance among the effects before the fluid crosses a boundary at the orifice of the nozzle and after it crosses that boundary. Before the fluid leaves the nozzle, the positive effect of the driving pressure gradient accelerates it, but energy losses due to viscous flow decelerate it. The kinetic energy with which it leaves the nozzle must be enough to cover the kinetic energy of the traveling fluid as well as the surface energy of the new free surface.

As indicated earlier, actuation energy is typically in the form of heating (bubble-jet) or vibration of a piezoelectric actuator. Various electrical energy waveforms may be used for actuation. In any event, these are standard types of inputs and will not be discussed further.

While the liquid to be ejected travels through the nozzle, before forming droplets, its motion is governed by the standard equations for incompressible, Newtonian fluids, as we are assuming these flows to be. The flow is fully described by the Navier–Stokes and continuity equations; however, these equations are difficult to solve analytically, so we will proceed with a simplification. The first term on the right side of (7.2) takes advantage of one situation for which an analytical solution is possible, that of steady, incompressible, laminar flow through a straight circular tube of constant cross section. The solution is the Hagen–Poiseuille law [62], which reflects the viscous losses due to wall effects:

$$\Delta p = \frac{8Q\mu l}{\pi r^4 \sigma} \quad (7.3)$$

where Q is the flow rate and r is the tube radius. Note that this expression is most applicable when the nozzle is a long, narrow glass tube. However, it can also apply when the fluid is viscous, as we will see shortly.

Another assumption made by using the Hagen–Poiseuille equation is that the flow within the nozzle is fully developed. For the case of laminar flow in a cylindrical pipe, the length of the entry region l_e where flow is not yet fully developed is defined as 0.06 times the diameter of the pipe, multiplied by the Reynolds number [62]:

Table 7.1 Entry lengths for “water” at various viscosities

Viscosity (cP)	Density (kg/m ³)	Entry length (μm)
1	1,000	240
	1,250	300
10	1,000	24
	1,250	30
40	1,000	6
	1,250	7.5
100	1,000	2.4
	1,250	3
200	1,000	1.2
	1,250	1.5

$$l_e = 0.06dRe = \frac{0.06\rho\bar{v}d^2}{\mu} \quad (7.4)$$

where \bar{v} is the average flow velocity across the pipe. To appreciate the magnitude of this effect, consider printing with a 20 μm nozzle in a plate that is 0.1 mm thick, where the droplet ejection speed is 10 m/s. The entry lengths for a fluid with the density of water and varying viscosities are shown in Table 7.1.

Entry lengths are a small fraction of the nozzle length for fluids with viscosities of 40 cP or greater. As a result, we can conclude that flows are fully developed through most of a nozzle for fluids that are at the higher end of the range of printable viscosities.

Most readers will have encountered the primary concepts of fluid mechanics in an undergraduate course and may be familiar with the Navier–Stokes equation, viscosity, surface tension, etc. As a reminder, viscosity is a measure of the resistance of a fluid to being deformed by shear or extensional forces. We will restrict our attention to dynamic, or absolute, viscosity, which has units of pressure-time; in the SI system, units are typically Pa · s or mPa s, for milli-Pascals-seconds. Viscosity is also given in units of poise or centipoises, named after Jean Louis Marie Poiseuille. Centipoise is abbreviated cP, which conveniently has the same magnitude as mPa s. That is, 1 cP is equal to 1 mPa s. Surface tension is given in units of force per length, or energy per unit area; in the SI system, surface tension often has units of N/m or J/m².

We can investigate the printing situation further by computing the pressures required for ejection. Equation (7.3) will be used to compute the pressure required to print droplets for various fluid viscosities and nozzle diameters. For many printing situations, wall friction dominates the forces required to print, hence we will only investigate the first term on the right of (7.2) and ignore the second and third terms (which are at least one order of magnitude smaller than wall friction).

Figure 7.13 shows how the pressure required to overcome wall friction varies with fluid viscosity and nozzle diameter. As can be seen, pressure needs to increase sharply as nozzles vary from 0.1 to 0.02 mm in diameter. This could be expected, given the quadratic dependence of pressure on diameter in (7.3). Pressure is seen to

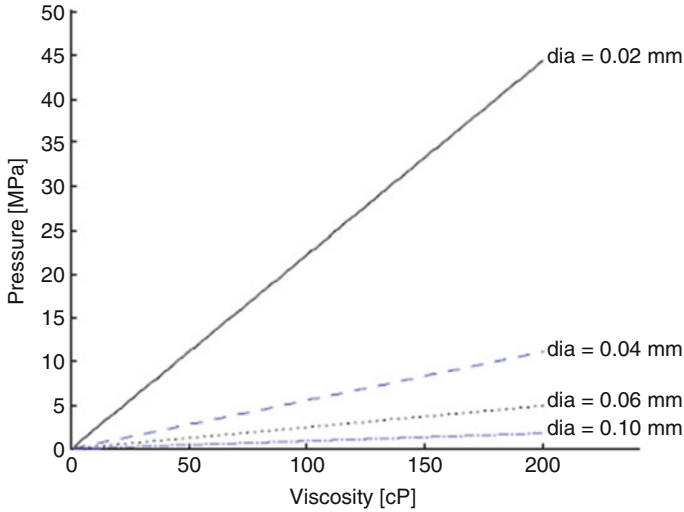


Fig. 7.13 Pressure required to overcome wall friction for printing through nozzles of different diameters

increase linearly with viscosity, which again can be expected from (7.3). As indicated, wall friction dominates for many printing conditions. However, as nozzle size increases, the surface tension of the fluid becomes more important. Also, as viscosity increases, viscous losses become important, as viscous fluids can absorb considerable acoustic energy. Regardless, this analysis provides good insight into pressure variations under many typical printing conditions.

Fluid flows when printing are almost always laminar; i.e., the Reynolds number is less than 2,100. As a reminder, the Reynolds number is

$$\text{Re} = \frac{\rho v r}{\mu} \quad (7.5)$$

Another dimensionless number of relevance in printing is the Weber number, which describes the relative importance of a fluid's inertia compared with its surface tension. The expression for the Weber number is:

$$\text{We} = \frac{\rho v^2 r}{\gamma} \quad (7.6)$$

Several research groups have determined that a combination of the Reynolds and Weber numbers is a particularly good indication of the potential for successful printing of a fluid [17]. Specifically, if the ratio of the Reynolds number to the square root of the Weber number has a value between 1 and 10, then it is likely that ejection of the fluid will be successful. This condition will be called the “printing indicator” and is

Table 7.2 Reynolds numbers and printing indicator values for some printing conditions

Nozzle diameter (mm)	Viscosity (cP)	Reynolds no.	Printing indicator
0.02	1	20	37.9
	10	2	3.79
	40	0.5	0.949
	100	0.2	0.379
0.05	1	50	60.0
	10	5	6.00
	40	1.25	1.50
	100	0.5	0.600
0.1	1	100	84.9
	10	10	8.49
	40	2.5	2.12
	100	1	0.849

$$1 \leq \frac{\text{Re}}{\text{We}^{1/2}} = \frac{\sqrt{\rho r \gamma}}{\mu} \leq 10 \quad (7.7)$$

The inverse of the printing indicator is another dimensionless number called the Ohnsorge number, that relates viscous and surface tension forces. Note that values of this ratio that are low indicate that flows are viscosity limited, while large values indicate flows that are dominated by surface tension. The low value of 1 for the printing indicator means that the maximum fluid viscosity should be between 20 and 40 cP.

Some examples of Reynolds numbers and printing indicators are given in Table 7.2. For these results, the surface tension is 0.072 N/m, the density is 1,000 kg/m³ (same as water at room temperature), and droplet velocity is 1 m/s.

It is important to realize that the printing indicator is a guide, not a law to be followed. Water is usually easy to print through most print heads, regardless of the nozzle size. But the printing indicator predicts that water (with a viscosity of 1 cP) should not be ejectable since its surface tension is too high. We will see in the next section how materials can be modified in order to make printing feasible.

7.5 Material Jetting Machines

The three main companies involved in the development of the RP printing industry are still the main players offering printing-based machines: Solidscape, 3D Systems, and Stratasys (after their merger with Objet Geometries). Solidscape sells the T66 and T612, both descendants of the previous ModelMaker line and based upon the first-generation melted wax technique. Each of these machines employs two single jets—one to deposit a thermoplastic part material and one to deposit a waxy support material—to form layers 0.0005 in. thick [63]. It should be noted that these machines also fly-cut layers after deposition to ensure that the layer

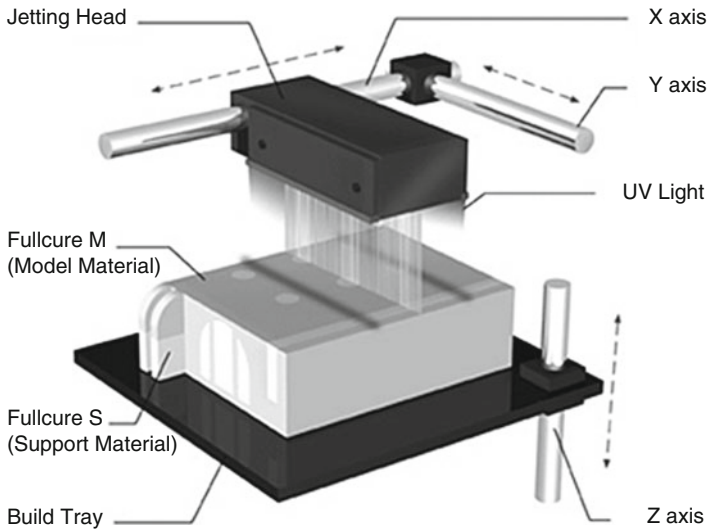


Fig. 7.14 Stratasys Polyjet build process [64]

is flat for the subsequent layer. Because of the slow and accurate build style as well as the waxy materials, these machines are often used to fabricate investment castings for the jewelry and dentistry industries.

3D Systems and Stratasys offer machines using the ability to print and cure acrylic photopolymers. Stratasys markets the Eden, Alaris, and Connex series of printers. These machines print a number of different acrylic-based photopolymer materials in 0.0006 in. layers from heads containing 1,536 individual nozzles, resulting in rapid, line-wise deposition efficiency, as opposed to the slower, point-wise approach used by Solidscape. Each photopolymer layer is cured by ultraviolet light immediately as it is printed, producing fully cured models without post-curing. Support structures are built in a gel-like material, which is removed by hand and water jetting [64]. See Fig. 7.14 for an illustration of Stratasys' Polyjet system, which is employed in all Eden machines. The Connex line of machines provides multimaterial capability. For several years, only two different photopolymers could be printed at one time; however, by automatically adjusting build styles, the machine can print up to 25 different effective materials by varying the relative composition of the two photopolymers. Machines are emerging that print increasing numbers of materials.

In competition with Stratasys, 3D Systems markets the ProJet printers, which print layers 0.0016 in. thick using heads with hundreds of nozzles, half for part material and half for support material [11]. Layers are then flashed with ultraviolet light, which activates the photoinitiated polymerization. The ProJets are the third generation of the Multi-Jet Modeling family from 3D Systems, following the ThermoJet described above and the InVision series. A comparison of the machines currently available is presented in Table 7.3.

Table 7.3 Commercially available printing-based AM machines [11, 63, 64]

Company/product	Cost (1000s)	Build size X × Y × Z (mm)	Min. layer (mm)	Resolution X, Y (dpi)	Material	Support
<i>SolidScap</i>						
3Z Studio	\$25	152 × 152 × 51	0.01	8,000 × 8,000	Wax-like	Soluble material
3Z Pro	\$46	152 × 152 × 102	0.01	8,000 × 8,000	"	"
<i>3D Systems</i>						
ProJet 3510 SD	\$60	298 × 185 × 203	0.032	375 × 375	Acrylate photopolymer (AP)	"
ProJet 3510 HD	\$78	298 × 185 × 203	0.029	750 × 750	AP	"
ProJet 3500 HDMax	\$92	298 × 185 × 203	0.016	750 × 750	AP	"
ProJet 3500 CPXMax	\$99	298 × 185 × 203	0.016	694 × 750	Wax-like	Wax
<i>Stratasys</i>						
Objet 24	\$20	240 × 200 × 150	–	–	AP	Gel-like photopolymer
Eden 250	\$60	255 × 252 × 200	0.028	600, 300	"	"
Eden 260V	\$90	250 × 250 × 200	0.016	600, 600	"	"
Eden 500V	\$170	490 × 390 × 200	0.016	600, 600	"	"
Connex500	\$240	490 × 390 × 200	0.016	600, 600	"	"
Objet 1000	\$500–700	1,000 × 800 × 500	0.016	600, 600	"	"

7.6 Process Benefits and Drawbacks

Each AM process has its advantages and disadvantages. The primary advantages of printing, both direct and binder printing, as an AM process include low cost, high speed, scalability, ease of building parts in multiple materials, and the capability of printing colors. Printing machines are much lower in cost than other AM machines, particularly the ones that use lasers. In general, printing machines can be assembled from standard components (drives, stages, print heads), while other machines have many more machine-specific components. High speed and scalability are related: by using print heads with hundreds or thousands of nozzles, it is possible to deposit a lot of material quickly and over a considerable area. Scalability in this context means that printing speed can be increased by adding another print head to a machine, a relatively easy task, much easier than adding another laser to a SL or SLS machine.

As mentioned, Stratasys markets the Connex machines that print in two or more part materials. One can imagine adding more print heads to increase the capability to many different materials and utilizing dithering deposition patterns raise the number of effective materials into the hundreds. Compatibility and resolution need to be ensured, but it seems that these kinds of improvements should occur in the near future.

Related to multiple materials, colors can be printed by some commercial AM machines (see Sect. 8.3). The capability of printing in color is an important advance in the AM industry; for many years, parts could only be fabricated in one color. The only exception was the selectively colorable SL resins that Huntsman markets for the medical industry, which were developed in the mid-1990s. These resins were capable of only two colors, amber and either blue or red. In contrast, two companies market AM machines that print in high resolution 24-bit color. Several companies are using these machines to produce figurines for video-gamers and other consumers (see Chaps. 3, 8, and 12).

For completeness, a few disadvantages of MJ will provide a more balanced presentation. The choice of materials to date is limited. Only waxes and photopolymers are commercially available. Part accuracy, particularly for large parts, is generally not as good as with some other processes, notably vat photopolymerization and material extrusion. However, accuracies have been improving across the industry and are expected to improve among all processes.

7.7 Summary

Each AM process has its advantages and disadvantages. The primary advantages of printing, both direct and binder printing, as an AM process include low cost, high speed, scalability, ease of building parts in multiple materials, and the capability of printing colors. Printing machines are lower in cost than many other AM machines, particularly the ones that use lasers or electron beams. In general, printing machines can be assembled from standard components (drives, stages, print heads), while

other machines have many more machine-specific components. Two primary mechanisms exist for droplet generation, continuous mode and DOD. At present, all commercial MJ machines utilize DOD print heads. High speed and scalability are related: by using print heads with hundreds or thousands of nozzles, it is possible to deposit a lot of material quickly and over a considerable area. Scalability in this context means that printing speed can be increased by adding another print head to a machine, a relatively easy task, much easier than adding another laser to a vat photopolymerization or powder bed fusion machine.

7.8 Exercises

1. List five types of material that can be directly printed.
2. According to the printing indicator (7.7), what is the smallest diameter nozzle that could be used to print a ceramic-wax material that has the following properties:
 - (a) Viscosity of 15 cP, density of $1,800 \text{ kg/m}^3$, and surface tension of 0.025 N/m .
 - (b) Viscosity of 7 cP, density of $1,500 \text{ kg/m}^3$, and surface tension of 0.025 N/m .
 - (c) Viscosity of 38 cP, density of $2,100 \text{ kg/m}^3$, and surface tension of 0.025 N/m .
3. Develop a build time model for a printing machine. Assume that the part platform is to be filled with parts and the platform is L mm long and W mm wide. The print head width is H mm. Assume that a layer requires three passes of the print head, the print head can print in both directions of travel (+ X and $-Y$), and the layer thickness is T mm. Figure 7.15 shows a schematic for the problem. Assume that a delay of D seconds is required for cleaning the print heads every K layers. The height of the parts to be printed is P mm.
 - (a) Develop a build time model using the variables listed in the problem statement.

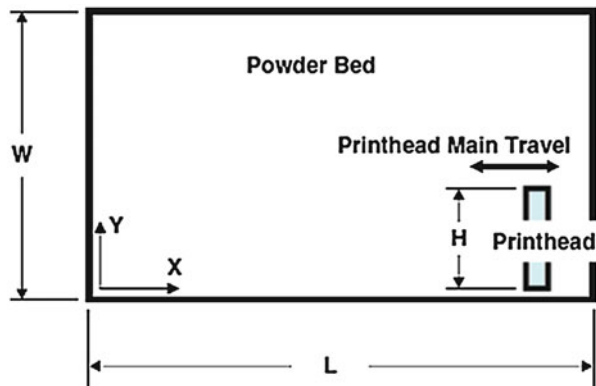


Fig. 7.15 Schematic for problems 4–5

Compute the build time for a layer of parts given the variable values in the following table.

	L	W	H	T	D	K	P
(b)	300	185	50	0.04	10	20	60
(c)	300	185	50	0.028	12	25	85
(d)	260	250	60	0.015	12	25	60
(e)	340	340	60	0.015	12	25	60
(f)	490	390	60	0.015	12	25	80

4. Modify the build time model from Problem 4 for the 3DP process. Assume that the powder bed recoating time is 10 s. Compute build times for a layer of parts using the values in Problem 4, assuming that layer thicknesses are 0.1 mm.
5. The integral in (7.2) can be evaluated analytically for simple nozzle shapes. Assume that the nozzle is conical with the entrance diameter of d_e and the exit diameter d_x .
 - (a) evaluate the integral analytically.

Use your integrated expression to compute pressure drop through the nozzle, instead of (7.3), for the following variable values:

	d_e (mm)	d_x (mm)	l (mm)	μ (cP)	ρ (kg/m ³)	γ (N/m)	v (m/s)
(b)	0.04	0.02	0.1	1	1,000	0.072	10
(c)	0.04	0.02	0.1	40	1,000	0.072	10
(d)	0.04	0.02	1.0	1	1,000	0.072	10
(e)	0.1	0.04	5.0	1	1,000	0.072	10
(f)	0.1	0.04	5.0	40	1,000	0.025	10

6. Using the integral from Problem 6, develop a computer program to compute pressure drop through the nozzle for various nozzle sizes and fluid properties. Compute and plot the pressure drop for the printing conditions of Fig. 7.14, but using nozzles of the following dimensions:
 - (a) $l = 0.1$ mm, $d_e = 0.06$ mm, $d_x = 0.02$ mm
 - (b) $l = 0.1$ mm, $d_e = 0.08$ mm, $d_x = 0.04$ mm
 - (c) $l = 0.1$ mm, $d_e = 0.12$ mm, $d_x = 0.05$ mm
 - (d) $l = 5.0$ mm, $d_e = 0.1$ mm, $d_x = 0.05$ mm

References

1. Le HP (1998) Progress and trends in ink-jet printing technology. *J Imaging Sci Technol* 42 (1):49–62
2. The rapid prototyping patent museum: basic technology patents. http://www.additive3d.com/museum/mus_c.htm. Accessed 17 Aug 2013
3. Wohlers T (2004) Wohlers report 2004. Wohlers Associates, Fort Collins
4. Derby B, Reis N (2003) Inkjet printing of highly loaded particulate suspensions. *MRS Bull* 28 (11):815–818

5. De Gans BJ, Duineveld PC, Schubert US (2004) Inkjet printing of polymers: state of the art and future developments. *Adv Mater* 16(3):203–213
6. MicroFab Technologies. MicroFab technote 99-02: fluid properties effects on ink-jet device performance. <http://www.microfab.com/equipment/technotes.html>
7. Paton A, Kruse J (1995) Reduced nozzle viscous impedance. US Patent 5,463,416
8. Gao F, Sonin AA (1994) Precise deposition of molten microdrops: the physics of digital fabrication. *Proc R Soc Lond A* 444:533–554
9. Reis N, Seerden KAM, Derby B, Halloran JW, Evans JRG (1999) Direct inkjet deposition of ceramic green bodies: II—jet behaviour and deposit formation. *Mater Res Soc Symp Proc* 542:147–152
10. Feng W, Fuh J, Wong Y (2006) Development of a drop-on-demand micro dispensing system. *Mater Sci Forum* 505–507:25–30
11. 3D Systems professional printers. <http://www.3dsystems.com/3d-printers/professional/overview>. Accessed 17 Aug 2013
12. Leyden R, Hull W (1999) Method for selective deposition modeling. US Patent 5,855,836
13. De Gans BJ, Kazancioglu E, Meyer W, Schubert US (2004) Ink-jet printing polymers and polymer libraries using micropipettes. *Macromol Rapid Commun* 25:292–296
14. Xu P, Ruatta S, Schmidt K, Doan V (2004) Phase change support material composition. US Patent 7,399,796
15. Schmidt K (2005) Selective deposition modeling with curable phase change materials. US Patent 6,841,116
16. Tay B, Edirisinghe MJ (2001) Investigation of some phenomena occurring during continuous ink-jet printing of ceramics. *J Mater Res* 16(2):373–384
17. Ainsley C, Reis N, Derby B (2002) Freeform fabrication by controlled droplet deposition of powder filled melts. *J Mater Sci* 37:3155–3161
18. Zhao X, Evans JRG, Edirisinghe MJ (2002) Direct ink-jet printing of vertical walls. *J Am Ceram Soc* 85(8):2113–2115
19. Wang T, Derby B (2005) Ink-jet printing and sintering of PZT. *J Am Ceram Soc* 88(8):2053–2058
20. Liu Q, Orme M (2001) High precision solder droplet printing technology and the state-of-the-art. *J Mater Process Technol* 115:271–283
21. Priest JW, Smith C, DuBois P (1997) Liquid metal jetting for printing metal parts. In: Solid freeform fabrication symposium, Austin, TX, 11–13 Aug, pp 1–9
22. Orme M (1993) A novel technique of rapid solidification net-form material synthesis. *J Mater Eng Perform* 2:399–405
23. Orme M, Huang C, Courter J (1996) Precision droplet-based manufacturing and material synthesis: fluid dynamics and thermal control issues. *Atomization Sprays* 6:305–329
24. Yamaguchi K (2003) Generation of 3-dimensional microstructure by metal jet. *Microsyst Technol* 9:215–219
25. Yamaguchi K, Sakai K, Yamanka T, Hirayama T (2000) Generation of three-dimensional micro structure using metal jet. *Precis Eng* 24:2–8
26. Liu Q, Orme M (2001) On precision droplet-based net-form manufacturing technology. *Proc Inst Mech Eng B J Eng Manuf* 215:1333–1355
27. Cao W, Miyamoto Y (2006) Freeform fabrication of aluminum parts by direct deposition of molten aluminum. *J Mater Process Technol* 173:209–212
28. Shimoda T, Morii K, Seki S, Kiguchi H (2003) Inkjet printing of light-emitting polymer displays. *MRS Bull* 28:821–827
29. Zhao X, Evans JRG, Edirisinghe MJ, Song JH (2001) Ceramic freeforming using an advanced multinozzle ink-jet printer. *J Mater Synth Proces* 9(6):319–327
30. Furbank RJ, Morris JF (2004) An experimental study of particle effects on drop formation. *Phys Fluids* 16(5):1777–1790
31. Bechtel SE, Bogy DB, Talke FE (1981) Impact of a liquid drop against a flat surface. *IBM J Res Dev* 25(6):963–971

32. Pasandideh-Fard M, Qiao Y, Chandra S, Mostaghimi J (1996) Capillary effects during droplet impact on a solid surface. *Phys Fluids* 8(3):650–659
33. Thoroddsen ST, Sakakibara J (1998) Evolution of the fingering pattern of an impacting drop. *Phys Fluids* 10(6):1359–1374
34. Bhola R, Chandra S (1999) Parameters controlling solidification of molten wax droplets falling on a solid surface. *J Mater Sci* 34:4883–4894
35. Attinger D, Zhao Z, Poulikakos D (2000) An experimental study of molten microdroplet surface deposition and solidification: transient behavior and wetting angle dynamics. *J Heat Transf* 122:544–556
36. Zhou W, Loney D, Fedorov AG, Degertekin FL, Rosen DW (2013) What controls dynamics of droplet shape evolution upon impingement on a solid surface? *AIChE J* 59(8):3071–3082
37. Bussman M, Chandra S, Mostaghimi J (2000) Modeling the splash of a droplet impacting a solid surface. *Phys Fluids* 12(12):3121–3132
38. Schiaffino S, Sonin AA (1997) Molten droplet deposition and solidification at low Weber numbers. *Phys Fluids* 9(11):3172–3187
39. Orme M, Huang C (1997) Phase change manipulation for droplet-based solid freeform fabrication. *J Heat Transfer* 119:818–823
40. Sanders R, Forsyth L, Philbrook K (1996) 3-D Model maker. US Patent 5,506,706
41. Thayer J, Almquist T, Merot C, Bedal B, Leyden R, Denison K, Stockwell J, Caruso A, Lockard M (2001) Selective deposition modeling system and method. US Patent 6,305,769
42. Gothait H (2005) System and method for three-dimensional model printing. US Patent 6,850,334
43. Gothait H (2001) Apparatus and method for three-dimensional model printing. US Patent 6,259,962
44. Bedal B, Bui V (2002) Method and apparatus for controlling the drop volume in a selective deposition modeling environment. US Patent 6,347,257
45. Tay B, Evans JRG, Edirisinghe MJ (2003) Solid freeform fabrication of ceramics. *Int Mater Rev* 48(6):341–370
46. MicroFab technote 99-01: background on ink-jet technology. <http://www.microfab.com/equipment/technotes/technote99-01.pdf>. Accessed 19 Mar 2006
47. Teng W, Edirisinghe MJ (1998) Development of continuous direct ink jet printing of ceramics. *Br Ceram Trans* 97(4):169–173
48. Blazdell PF, Evans JRG, Edirisinghe MJ, Shaw P, Binstead M (1995) The computer aided manufacture of ceramics using multilayer jet printing. *J Mater Sci Lett* 54:1562–1565
49. Blazdell PF (2003) Solid free-forming of ceramics using a continuous jet printer. *J Mater Process Technol* 137:49–54
50. Tseng AA, Lee MH, Zhao B (2001) Design and operation of a droplet deposition system for freeform fabrication of metal parts. *J Eng Mater Technol* 123:74–84
51. Basaran OA (2002) Small-scale free surface flows with breakup: drop formation and emerging applications. *AIChE J* 48(9):1842–1848
52. Siringhaus H, Kawase T, Friend RH, Shimoda T, Inbasekaran M, Wu W, Woo EP (2000) High-resolution inkjet printing of all-polymer transistor circuits. *Science* 290:2123–2126
53. Lee E (2002) *Microdrop generation*. CRC Press, Boca Raton
54. Percin G, Khuri-Yakub BT (2002) Piezoelectrically actuated flextensional micromachined ultrasound droplet ejectors. *IEEE Trans Ultrason Ferroelectr Freq Control* 49(6):756–766
55. Elrod SA, Hadimioglu B, Khuri-Yakub BT, Rawson EG, Richley E, Quate CF (1989) Nozzleless droplet formation with focused acoustic beams. *J Appl Phys* 65(9):3441–3447
56. Meacham JM, Ejimofor C, Kumar S, Degertekin FL, Fedorov AG (2004) Micromachined ultrasonic droplet generator based on a liquid horn structure. *Rev Sci Instrum* 75(5):1347–1352
57. Meacham JM, Varady M, Degertekin FL, Fedorov AG (2005) Droplet formation and ejection from a micromachined ultrasonic droplet generator: visualization and scaling. *Phys Fluids* 17:100605
58. Margolin L (2006) Ultrasonic droplet generation jetting technology for additive manufacturing: an initial investigation. MS Thesis, Georgia Institute of Technology

59. Fukumoto H, Aizawa J, Nakagawa H, Narumiya H (2000) Printing with ink mist ejected by ultrasonic waves. *J Imaging Sci Technol* 44(5):398–405
60. Meacham JM, O'Rourke A, Yang Y, Fedorov AG, Degertekin FL, Rosen DW (2010) Experimental characterization of high viscosity droplet ejection. *J Manuf Sci E-T ASME* 132(3):030905
61. Sweet R (1964) High-frequency oscillography with electrostatically deflected ink jets. SEL-64-004, SELTR17221. Stanford Electronics Laboratories, Stanford, CA
62. Munson B, Young D, Okiishi T (1998) *Fundamentals of fluid mechanics*, 3rd edn. Wiley, New York
63. Solidscape. T66 Benchtop: product description. <http://www.solid-scape.com/t66.html>. Accessed 31 July 2006
64. Stratasys Polyjet Technology. <http://stratasys.com/3d-printers/technology/polyjet-technology>. Accessed 17 Aug 2013